01 Jan 1986

CHARACTERIZATION OF MODE I AND MIXED-MODE FAILURE OF ADHESIVE BONDS BETWEEN COMPOSITE ADHERENDS.

S. Mall

Walter Johnson
Missouri University of Science and Technology

Recommended Citation

Mall, S., & Johnson, W. (1986). CHARACTERIZATION OF MODE I AND MIXED-MODE FAILURE OF ADHESIVE BONDS BETWEEN COMPOSITE ADHERENDS.. *ASTM Special Technical Publication*, pp. 322-334. ASTM.
The definitive version is available at https://doi.org/10.1520/stp35356s

S. Mall[1] *and W. S. Johnson*[2]

Characterization of Mode I and Mixed-Mode Failure of Adhesive Bonds Between Composite Adherends

REFERENCE: Mall, S. and Johnson, W. S., **"Characterization of Mode I and Mixed-Mode Failure of Adhesive Bonds Between Composite Adherends,"** *Composite Materials: Testing and Design (Seventh Conference)*, *ASTM STP 893*, J. M. Whitney, Ed., American Society for Testing and Materials, Philadelphia, 1986, pp. 322–334.

ABSTRACT: A combined experimental and analytical investigation of an adhesively bonded composite joint was conducted to characterize both the static and fatigue debond growth mechanism under Mode I and Mixed-Mode I and II loadings. Two bonded systems were studied: graphite/epoxy adherends bonded with EC 3445 and FM-300 adhesives. For each bonded system, two specimen types were tested: (1) a double-cantilever-beam specimen for Mode I loading and (2) a cracked-lap-shear specimen for Mixed-Mode I and II loading. In all specimens tested, failure occurred in the form of debond growth. Debonding always occurred in a cohesive manner with EC 3445 adhesive. The FM-300 adhesive debonded in a cohesive manner under Mixed-Mode I and II loading, but in a cohesive, adhesive, or combined cohesive and adhesive manner under Mode I loading. Total strain-energy release rate appeared to be the driving parameter for debond growth under static and fatigue loadings.

KEY WORDS: composite materials, adhesive bonding, debond propagation, strain-energy release rates, fracture mechanics, fatigue (materials)

Nomenclature

a Length of debond, mm
A_1, A_2 Constants from least square fit
$\frac{da}{dN}$ Debond growth rate, mm/cycle.
C Compliance, mm/N
c Curve-fit parameters for power-law equation
G_I Mode I strain-energy release rate, J/m^2

[1]Associate professor, Department of Engineering Mechanics, University of Missouri, Rolla, MO 65401.

[2]Research engineer, National Aeronautics and Space Administration, Langley Research Center, Hampton, VA 23665.

G_{Ic} Fracture toughness, J/m^2
G_{II} Mode II strain-energy release rate, J/m^2
G_T Total strain-energy release rate ($G_I + G_{II}$), J/m^2
G_{Tc} Critical total strain-energy release rate, J/m^2
N Number of cycles
n Curve-fit parameter for power-law equation
P_{cr} Critical load, N
w Width of specimen, mm

To achieve the maximum saving in weight without sacrificing strength, engineers are faced with the problem of developing methods of joining structural composite components without weakening or damaging them. It is impossible to use conventional fastening techniques without drastically affecting the strength of fiber-reinforced composites. Hence, adhesive bonding is a desirable alternative to mechanical fastening in composite structures. Even with all the potential advantages and encouraging experience with adhesive bonding, manufacturers still hesitate to use this technology in primary structural components. This reluctance is due, in part, to the lack of understanding of failure mechanism and durability. Several studies have been reported on the static strength of adhesively bonded composite joints (for example, see Refs *1–3*); however, very little information is available on their fatigue behavior.

The possible fatigue failure modes for bonded composites are: cyclic debonding (namely, progressive separation of the adhesive bond under cyclic load), cyclic delamination, adherend fatigue, or a combination of these. In a previous study [*4*], cyclic debonding of adhesively bonded composites was investigated under a mixed-mode loading, which introduced a combination of opening (Mode I) and sliding (Mode II) at the debond front. Graphite/epoxy (T300/5208) cracked-lap-shear (CLS) specimens were tested under constant amplitude cyclic loading in an ambient laboratory environment. Two adhesives were used: EC 3445 and FM-300. A fracture mechanics approach, employed previously in fatigue studies of composite-to-metal joints [*5,6*] and metal-to-metal joints [*7,8*], was used to model the cyclic debonding. The strain-energy release rate associated with cyclic failure of the adhesive bond was correlated with the measured cyclic debond growth rate, da/dN. Two different geometries of the CLS specimens were tested. These two specimen geometries provided the different ratio of G_I/G_{II}, where G_I and G_{II} are the strain-energy release rates for opening Mode I and for sliding Mode II, respectively. Data from these two specimens were used to determine fracture mode dependence of the adhesive. The cyclic debond growth rate correlated better with the total strain-energy release rate, G_T, than it did with either G_I or G_{II} independently [*4*].

Since the previous study [*4*] was based on a rather narrow range of G_I/G_{II} ratios (that is, 0.25 to 0.38), further investigations were required to substantiate that G_T is the cyclic debond driver for tough structural adhesives. The previously

tested CLS specimens produced mostly shear stresses at the debond tip, therefore, this study will address a specimen configuration that is entirely loaded in peel (namely, G_I), the double-cantilever-beam specimen (DCB). Also, the previous study focused solely on cyclic debonding. The present study included static toughness results as well as cyclic results from the CLS and DCB specimens to evaluate the mixed-mode loading effects. The data obtained from both CLS and DCB specimens gave a very wide range of mixed-mode loading conditions for evaluation.

Specimen Preparation and Configuration

Two bonded systems were studied: graphite/epoxy (T300/5208) adherends bonded with either EC 3445 adhesive or with FM-300 adhesive [*9*]. The EC 3445 adhesive is a thermosetting paste with a cure temperature of 121°C; specimens were fabricated by conventional secondary bonding procedures. The FM-300 is a modified epoxy adhesive supported with a carrier cloth with a cure temperature of 177°C. The FM-300 specimens were fabricated by cocure, whereby adherends were cured and bonded simultaneously. The bonding processes followed the manufacturers' recommended procedures for each adhesive. The nominal adhesive thickness was 0.10 mm and 0.25 mm for the EC 3445 and FM-300, respectively.

Two specimen types were fabricated: DCB specimens and CLS specimens. The DCB and CLS specimens (shown in Figs. 1 and 2) were used to characterize debond growth under opening Mode I loading and the mixed-mode loading, respectively. The DCB specimen consisted of two bonded adherends, each having 14 unidirectional plies with an initial debond of 38-mm length. This debond was introduced by a Teflon film of thickness equal to the adhesive bondline. Two 0.5-mm-thick aluminum end tabs were bonded to the DCB specimen, along with two 1.3-mm-thick aluminum reinforcing plates. The peeling load was applied through these tabs.

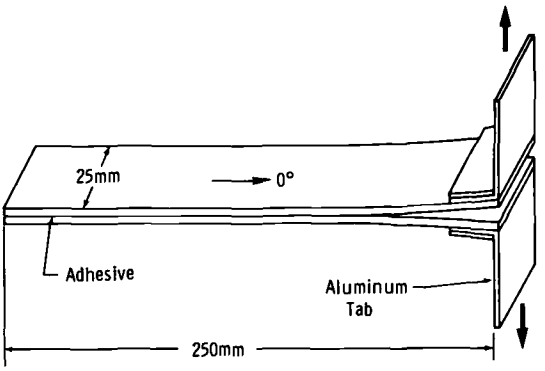

FIG. 1—*Double-cantilever-beam (DCB) specimen.*

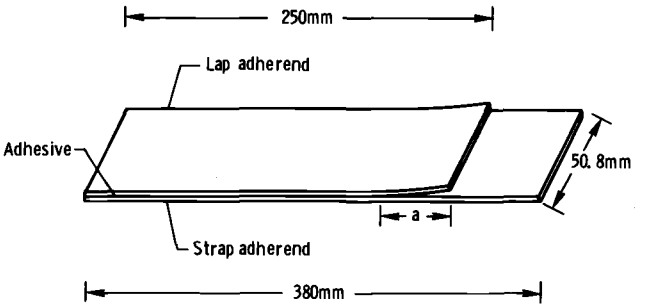

FIG. 2—*Cracked-lap-shear (CLS) specimen.*

The adherends of the cracked-lap-shear specimens consisted of quasi-isotropic lay-ups, $[0/45/-45/90]_s$ and $[0/45/-45/90]_{2s}$. Two configurations of CLS specimens were tested: 8-ply strap to 16-ply lap and 16-ply strap to 8-ply lap. The two adhesive systems with these two geometries resulted in four sets of specimens. The CLS specimen did not have an initial debond like the DCB specimens.

Testing Procedure

The test program included the static and fatigue tests for both types of specimens. The objective of the test program was to measure the critical strain-energy release rate under the static loading, and to measure the debond growth rate under the cyclic loading. These are described separately for each specimen in the following paragraphs.

Static Tests of DCB Specimen

All static tests of DCB specimens were performed in a displacement-controlled test machine. Both edges of the specimen were coated with a white brittle fluid, to aid in visually locating the debond tip. Fine visible marks were put on these edges, at 1-mm intervals, to aid in measuring the debond length. The debond length was measured visually on both sides with two microscopes having a magnification factor of 20. Prior to testing, either for static or fatigue loading, these specimens were fatigued to create a debond of at least 6 mm beyond the end of Teflon film. The static test involved the application of displacement at a slow crosshead speed (approximately 1.0 mm/min). The load corresponding to the applied displacement was also recorded. When the load reached the critical value, the debond grew. The onset of growth results in a deviation from linearity in the load versus crosshead displacement record. The applied displacement was then decreased until a zero load reading was observed. After each static test, the specimen was fatigued until the debond grew at least 6 mm further, thus forming a sharp crack for the next static test. A series of static tests was performed on each specimen, which provided compliance and critical load measurements at

several debond lengths. These measurements provided the critical strain-energy release rate as explained in the Results and Discussions section of this paper.

Fatigue Tests of DCB Specimen

The fatigue tests of DCB specimens were conducted in a servohydraulic test machine at a cyclic frequency of 3 Hz. Two constant-amplitude testing modes were employed: (1) constant-amplitude cyclic load and (2) constant-amplitude cyclic displacement. In both modes, the ratio of minimum to maximum load (or displacement) in a fatigue cycle was 0.1. In displacement-controlled tests, debond growth rates reduced as the debond propagated, while in the case of load-controlled tests, debond growth rates increased as the debond propagated. Debond lengths, fatigue cycles, applied loads, and displacements were monitored continuously throughout each test. The measured relationship between the debond length and fatigue cycle provided the debond growth rate, da/dN. The strain-energy release rate, G_I, was computed from the measured compliance and applied load, as explained in the Results and Discussions section. Thus, a relationship between G_I and da/dN was established for the cyclic debonding under Mode I loading.

Static Tests of CLS Specimen

Static tension tests on CLS specimens were conducted in a displacement-controlled mode. Prior to static testing, this specimen was fatigued, and thus it had an initial sharp debond. During the test, the axial load and displacement were recorded. The displacement was measured with two displacement transducers attached on the opposite sides of the specimen. The applied load was increased slowly until the debond propagated. The critical load corresponding to unstable debond growth was measured and verified by the deviation from linearity in the recorded load-displacement curve. Only one such measurement could be obtained from each specimen, since debonds grew into the composite strap adherend. Static tests were conducted on all four sets of specimens (that is, two geometries and two adhesives).

Fatigue Tests of CLS Specimen

A detailed investigation of cyclic debonding under mixed-mode loading was conducted in a previous study [*4*]. In that study, the CLS specimen was tested under constant-amplitude cyclic load at 10 Hz frequency and stress ratio, $R = 0.1$. In the present study, fatigue tests of the CLS specimen were conducted at 3 Hz in order to compare mixed-mode results with Mode I results from DCB specimens that were also obtained at 3 Hz frequency. Only the 8-ply strap bonded to the 16-ply lap with EC 3445 adhesive system was tested at 3 Hz.

Analysis

Static tests on DCB specimens, conducted as described earlier, provided the critical load, P_{cr}, and the compliance, C, for each debonded length. The measured values of P_{cr} and C were used with linear beam theory to compute the fracture toughness, G_{Ic}. The details of this procedure are elaborated by Wilkins et al [*10*]. A brief description of the Wilkins et al technique is given subsequently. Figure 3 shows the variation of compliance with the debond length in a typical DCB specimen with EC 3445 adhesive. A compliance relationship of

$$C = A_1 a^3 \tag{1}$$

was fitted through the experimental data points by the method of least squares that is shown in Fig. 3 as a solid line. This relationship, based on linear beam theory, fits very well with the experimental data. The constant, A_1, in Eq 1 is $2/3EI$, where E is the extensional stiffness and I is the moment of inertia of each adherend of the DCB specimen. The experimental values of A_1 are $\pm 7\%$ of the linear beam theory value of 3.77×10^{-7}.

Finite-element analysis [*11*] was also used to analyze the DCB results. The adhesive was modeled with eight layers of elements. The analysis was conducted assuming plane-strain conditions. The experimental values of compliance were within $\pm 5\%$ of those given by a geometric linear finite-element analysis. The computer compliances at several debond lengths were within 5% of the experimental values. These computed values are also shown in Fig. 3. Further, the geometric nonlinear analysis of this specimen did not show any significant change from the linear analysis. The maximum difference in the computed compliance from nonlinear and linear analyses was 5% for the maximum debond length

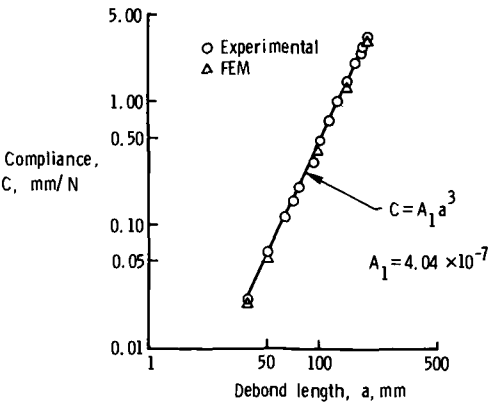

FIG. 3—*Relationship between compliance and debond length for a DCB specimen with EC 3445 adhesive.*

employed in the investigation (that is, 200 mm) at its maximum or critical load. Thus, the compliance-debond length relationship, expressed by Eq 1, represents the appropriate behavior of the presently employed DCB specimen. All results from the DCB specimen in this study are calculated using the linear beam theory.

Figure 4 shows the measured critical load as a function of debond length for a typical specimen with EC 3445 adhesive. Based on the linear beam theory [*10*], a relationship between the critical load, P_{cr}, and the debond length, a, is

$$P_{cr} = A_2/a \tag{2}$$

A solid line shown in Fig. 4 with a slope of -1 was fitted to the experimental data with the method of least squares. Then, the averaged value of G_{Ic} for each specimen was computed from the relationship

$$G_{Ic} = \frac{P_{cr}^2}{2w}\frac{\partial C}{\partial a} = 3A_1A_2^2/(2w) \tag{3}$$

where w is the specimen width. A similar procedure was used to compute the strain-energy release rate, G_I, associated with the cyclic debonding where the critical load was replaced by the maximum load of the fatigue cycle. The details of the analysis for the CLS specimens are given in Ref *4*.

Results and Discussions

Debond Locations

All DCB and CLS specimens with both adhesives EC 3445 and FM-300 failed by debond propagation during both static and fatigue tests. However, the debond grew in a different manner in each case. In the case of DCB specimens with EC

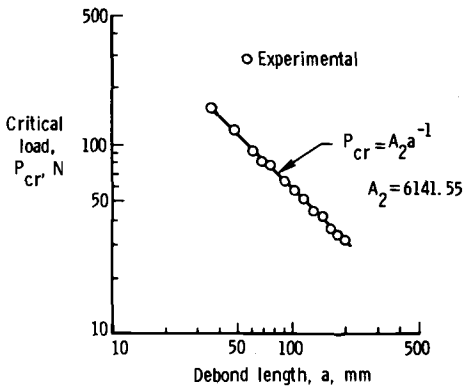

FIG. 4—*Relationship between critical load and debond length for a DCB specimen with EC 3445 adhesive.*

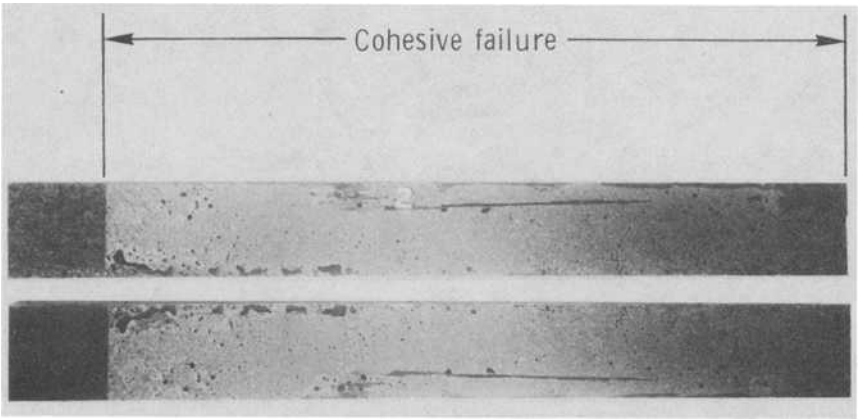

FIG. 5—*Debonded surfaces of DCB specimen with EC 3445 adhesive.*

3445 adhesives, the debond grew in a cohesive manner during both static and fatigue tests. Here the debond grew consistently in the middle portion of the adhesive layer. In DCB specimens with FM-300, the debond propagated in an irregular manner during both static and fatigue tests, involving cohesive, adhesive, or mixed cohesive-adhesive debonding. Typical debonded surfaces with these failure details are shown in Figs. 5 and 6 for both adhesives.

The CLS specimens debonded in a cohesive manner during fatigue tests for both adhesive systems. The debond grew in the vicinity of strap-adhesive interface. A possible explanation of this phenomenon is given in the previous study [*4*].

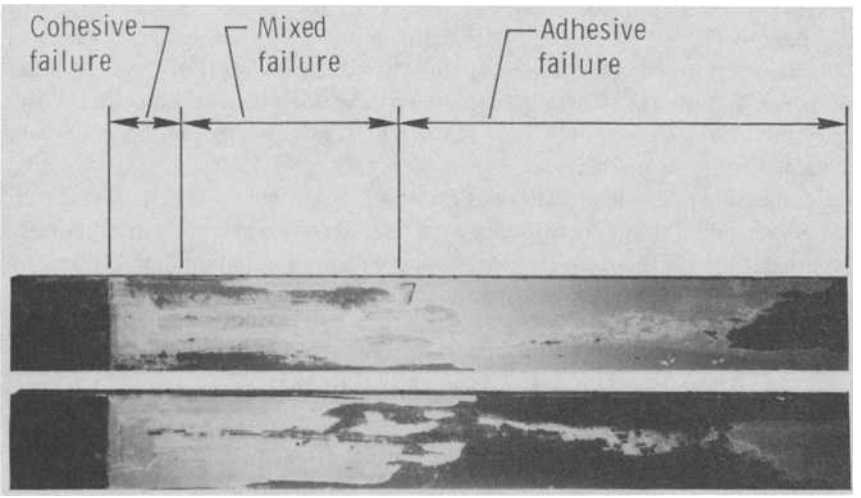

FIG. 6—*Debonded surfaces of DCB specimen with FM-300 adhesive.*

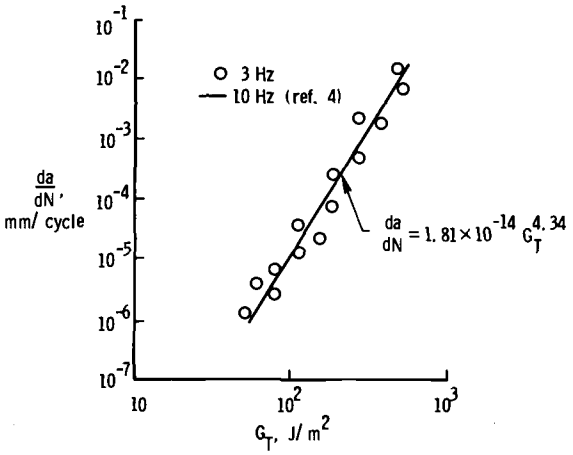

FIG. 7—*Relationship between total strain-energy release rate and debond growth rate of EC 3445 adhesive at two cyclic frequencies using CLS specimens.*

Cyclic Debonding Behavior

In the present study, all fatigue tests with both DCB and CLS specimens were conducted at 3 Hz. Figure 7 shows the comparison between the G_T versus da/dN relationship for two cyclic frequencies, 10 Hz and 3 Hz, obtained from CLS specimens with EC 3445 adhesive. The solid line shown is a power-law relationship

$$da/dN = cG_T^n. \tag{4}$$

which was obtained in the previous study [*4*] by the method of least square fit to experimental data at 10 Hz, while the data in Fig. 7 correspond to the 3 Hz cyclic test performed in the present study. The scatter in data is of the same order as obtained at 10 Hz (which is not shown here for the sake of clarity). The relationship between G_T and da/dN is, therefore, not affected by this change in frequency from 10 Hz to 3 Hz.

The measured debond growth rates from DCB specimens were correlated with the corresponding strain-energy release rate, G_I, as shown in Fig. 8. As previously mentioned, the DCB specimens were tested with constant-amplitude cyclic load and constant-amplitude cyclic displacement. Data obtained from these two testing modes are shown in Fig. 8. The constant load testing results in G increasing with debond length while the constant displacement results in G decreasing. Since the constant displacement tests resulted in faster debond rates, the debond process appears to be influenced by the G gradient. Figure 8 also shows G_T versus da/dN and G_I versus da/dN relationships from the CLS specimens under mixed-mode loading [*4*]. The scatter in data from the DCB specimens was larger than from the CLS specimens. The CLS data points [*4*] are not shown herein for the

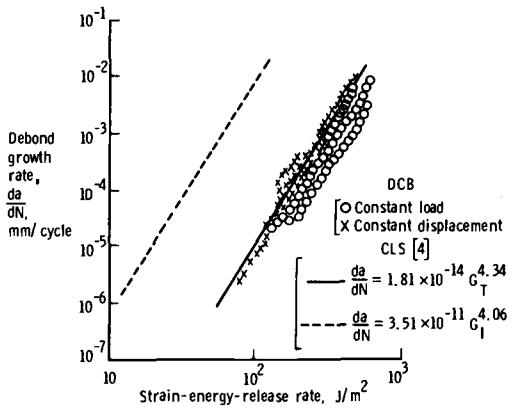

FIG. 8—*Relationship between strain-energy release rates and debond growth rate of EC 3445 adhesive for DCB and CLS specimens.*

sake of clarity. The G_I versus *da/dN* data from the DCB specimen are in good agreement with the G_T versus *da/dN* relationship from the CLS specimen, represented by the solid line. On the other hand, the G_I versus *da/dN* relationship from the CLS specimen represented by the dashed line, did not agree with the DCB specimen. This indicates that the cyclic debond growth is a function of total strain-energy release rate.

A similar phenomenon was also observed in the case of FM-300 adhesive. Figure 9 shows the comparison of the G_T versus *da/dN* relationship from the DCB specimen. The data shown from the DCB specimen were obtained under the constant-amplitude cyclic displacement. As previously mentioned, cyclic debonding occurred in cohesive manner, adhesive manner, or a combination of both in the DCB specimens. In Fig. 9, data on the right-hand side correspond to the cohesive failure, and data in between these correspond to the mixed failure.

Static Debonding Behavior

Figure 10 shows the critical strain-energy release rates, G_{Tc} and G_{Ic}, obtained from static tests of CLS and DCB specimens, respectively. The total critical strain-energy release rate, G_{Tc}, from the CLS specimen is in agreement with fracture toughness, G_{Ic}, from DCB specimen in each case. This shows that the total critical strain-energy release is also the driving parameter for debond growth during static loading. The only exceptions are those adhesive failures in the FM-300 DCB specimens. These adhesive failure strengths are 40% lower than the cohesive failure strengths.

General

The cyclic debond growth rate data show, in each case, that the debond propagates at G_T values as much as an order of magnitude below the critical

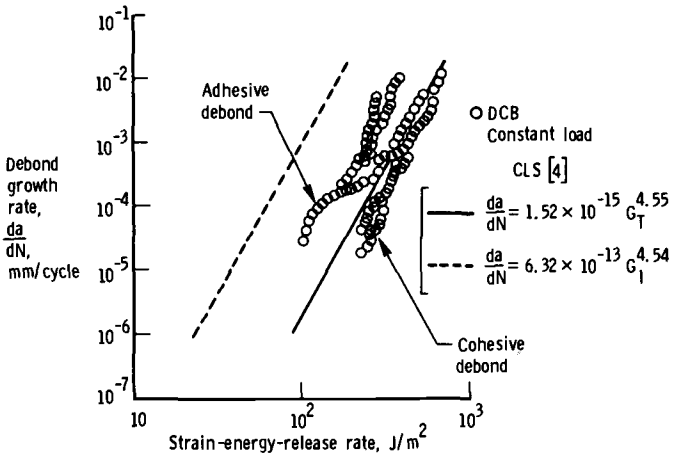

FIG. 9—*Relationship between strain-energy release rates and debond growth rate of FM-300 adhesive for DCB and CLS specimens.*

static value. So static data alone are insufficient for safe joint design. Instead, the G_T associated with cyclic debonding at very slow growth rates is more appropriate as a design value and as a criterion for adhesive selection. The threshold value of G_T has been demonstrated as a viable fracture mechanics approach for designing the adhesive joint [*12*]. If the total strain-energy release rate is a governing parameter for the cyclic debond initiation and propagation, as results of the present and previous studies [*4,12*] have shown, then it would require the characterization of cyclic debonding under Mode I loading only. It would be simpler and easier than testing under mixed-mode loading. This should be, however, verified further for several structural adhesives and various loading conditions. It is suspected that only relatively tough adhesives would demonstrate a G_T governed debond behavior.

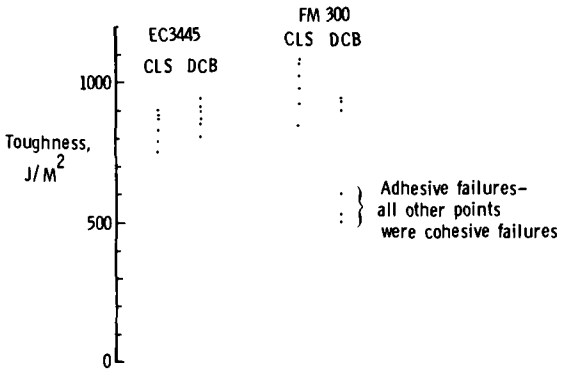

FIG. 10—*Static toughness of FM-300 and EC 3445 adhesives derived from DCB and CLS specimens.*

The G_T is much easier to calculate than are the individual G_I and G_{II} components of a mixed-mode specimen. The G_T can be measured directly from most laboratory specimens. Therefore, even if some error is involved with using G_T as a design parameter, as in Ref [*12*], the ease of calculation may compensate.

Concluding Remarks

A combined experimental and analytical investigation of composite-to-composite bonded joints was undertaken to characterize the debond growth mechanism under Mode I and Mixed-Mode I and II static and fatigue loadings. Two bonded systems were studied: graphite/epoxy adherends bonded with EC 3445 adhesive and with FM-300 adhesives. With each bonded system, two specimen types were tested: (1) a double-cantilever-beam specimen for Mode I loading and (2) a cracked-lap-shear specimen for Mixed-Mode I and II loadings. The following conclusions were obtained.

1. The total strain-energy release rate, G_T, appears to be the governing parameter for cohesive debond growth under static and fatigue loadings. This is indeed significant since in most cases G_T is much easier to calculate or determine experimentally than are G_I and G_{II} components of a mixed-mode specimen.
2. Debond growth was measured at G_T values that were an order of magnitude below the static toughness, G_{Tc}. Therefore, one needs to consider both debond growth threshold values as well as static strength in design and material development and selection.

References

[*1*] Matthews, F. L., Kilty, P. F., and Godwin, E. W., *Composites*, Vol. 13, No. 1, 1982, pp. 29–37.

[*2*] Hart-Smith, L. J., "Analysis and Design of Advanced Composite Bonded Joints," NASA CR-2218, National Aeronautics and Space Administration, 1974.

[*3*] Renton, W. J. and Vinson, J. R., "The Analysis and Design of Composite Material Bonded Joints Under Static and Fatigue Loadings," AFOSR-TR-72-1627, U. S. Air Force, 1973.

[*4*] Mall, S., Johnson, W. S., and Everett, R. A., Jr., "Cyclic Debonding of Adhesively Bonded Composites," NASA TM-84577, National Aeronautics and Space Administration, Nov. 1982; also in *Adhesive Joints: Their Formation, Characteristics, and Testing*, K. L. Mittal, Ed., Plenum Press, New York, 1984.

[*5*] Roderick, G. L., Everett, R. A., Jr., and Crews, J. H., Jr., in *Fatigue of Composite Materials, ASTM STP 569*, American Society for Testing and Materials, Philadelphia, 1975, pp. 295–306.

[*6*] Everett, R. A., Jr., "The Role of Peel Stresses in Cyclic Debonding," NASA TM-84504, National Aeronautics and Space Administration, 1982.

[*7*] Brussat, T. R., Chiu, S. T., and Mostovoy, S., "Fracture Mechanics for Structural Adhesive Bonds," AFML-TR-1963, Air Force Materials Laboratory, 1977.

[*8*] Romanko, J. and Knauss, W. G., "Fatigue Behavior of Adhesively Bonded Joints," Vol. I, AFWAL-TR-80-4037, U. S. Air Force, 1980.

[*9*] Alsmiller, G. R., Jr., and Anderson, W. P., "Advanced Composites Airframe Program—Preliminary Design," USAAVRADCOM-TR-80-D-37A, U. S. Army, 1982.

[*10*] Wilkins, D. J., Eisenmann, J. R., Camin, R. A., Margolis, W. S., and Benson, R. A. in *Damage in Composite Materials, ASTM STP 775*, K. Reifsnider, Ed., American Society for Testing and Materials, Philadelphia, 1981, pp. 168–183.

[*11*] Dattaguru, B., Everett, R. A., Jr., Whitcomb, J. D., and Johnson, W. S., "Geometrically-Nonlinear Analysis of Adhesively Bonded Joints," NASA TM-84562, National Aeronautics and Space Administration, 1982.

[*12*] Johnson, W. S. and Mall, S., "A Fracture Mechanics Approach for Designing Adhesively Bonded Joints," NASA TM-85694, National Aeronautics and Space Administration, Sept. 1983.